## Supporting Information

# Dimeric and 1D polymeric low-chlorinated $C_{60}$ fullerenes, $(C_{60}Cl_5)_2$ and $(C_{60}Cl_4)_\infty$

**Victor A. Brotsman, Nadezhda B. Tamm, Ilya N. Ioffe, Andrei A. Eliseev, Alexey A. Goryunkov, Konstantin A. Lyssenko and Sergey I. Troyanov**

***Moscow State University, Chemistry Department, Leninskie gory,119991 Moscow, Russia***

### Isolation and characterization of the products of chlorination

Chlorination of $C_{60}$ was carried out in thick-walled glass ampoules. 50 mg $C_{60}$ and a predefined amount of metallic antimony were placed into an ampoule which was then evacuated and filled with inert gas. Then ca. 0.25 mL (590–600 mg) of $SbCl_5$ was added, the ampoule was once again evacuated under cooling and sealed off. The amount of metallic Sb, typically in the range of 80 to 110 mg, was chosen to give a predefined $SbCl_5/(SbCl_3 + SbCl_3)$ mole fraction after complete transformation of $C_{60}$ into $C_{60}Cl_6$ and Sb into $SbCl_3$. In the two main experiments, batches B1 and B2, the said final mole fractions were, respectively, 0.30 and 0.22. In some other experiments (B3), the ratio was below 0.20. It should be noted that exothermic interaction of Sb with $SbCl_5$ begins immediately after addition of the latter. During the ampoule heating in a temperature gragient, most $SbCl_5$ is concentrated in the gas phase, thus leaving the liquid phase enriched with $SbCl_3$.

The reaction ampoules were heated in a tube furnace at 270 °C for 1–2 weeks. After cooling to the room temperature and opening, their content was heated to 100–150 °C under vacuum to remove the excess of $SbCl_5$ and $SbCl_3$ from the reaction products. An alternative way to remove the antimony chlorides from the reaction products involves treatment with conc. HCl, then with dilute HCl and water. The chlorination products were then dried under vacuum at gentle heating. The analysis of the chlorination products was normally performed with MALDI TOF mass spectrometry, HPLC-MS, and, whenever any crystals of suitable size and quality were available, single crystal X-ray diffraction. According to the analyses, the main product in the batches B1 and B2 was $(C_{60}Cl_5)_2$ (yields about 80–85%) which is insoluble in organic solvents. The impurities were mainly soluble highly-chlorinated fullerenes removable by washing with toluene. The products were characterized with X-ray diffraction, IR and Raman spectrometry, and EDX. In several batches with lower concentration of $SbCl_5$ (m = 0.13–0.18), the main chlorination product was similarly insoluble, but X-ray diffraction revealed the presence of polymeric $(C_{60}Cl_4)_\infty$ co-crystallized with $SbCl_3$ in a 1:1 ratio. Thermal behavior of the polymeric phase was studied in the range of up to 500 °C.

### X-ray crystallography

Data collection for single crystals of $(C_{60}Cl_5)_2$ and $(C_{60}Cl_4)_\infty$ was performed at, respectively, 106 and 110 K on a Bruker D8 Quest diffractometer ($\lambda$ = 0.71073 Å). All structures were solved and anisotropically refined using the SHELX package. Selected crystallographic data, details of data collection and refinement, and CCDC deposition numbers are given in Table S1.

**Table *S*1**. Selected crystallographic data and some details of data collection and refinement.

| **Compound** | **$(C_{60}Cl_5)_2$ (B1)** | **$(C_{60}Cl_5)_2$ (B2)** | **$(C_{60}Cl_4)_\infty$** |
|---|---|---|---|
| Solvent | - | - | $SbCl_3$ |
| $M_r$ | 1795.70 | 1795.70 | 1090.50 |
| crystal system | orthorhombic | orthorhombic | monoclinic |
| space group | *Pca2₁* | *Pca2₁* | *P*2₁ |
| $a$ [Å] | 19.474(3) | 19.4815(9) | 11.919(2) |
| $b$ [Å] | 11.2064(16) | 11.2123(6) | 12.101(2) |
| $c$ [Å] | 28.978(4) | 28.9836(18) | 12.228(2) |
| $\alpha$ [°] | 90 | 90 | 90 |
| $\beta$ [°] | 90 | 90 | 104.11(3) |
| $\gamma$ [°] | 90 | 90 | 90 |
| $V$ [Å$^3$] | 6324.0(15) | 6331.0(6) | 1710.3(6) |
| $Z$ | 4 | 4 | 2 |
| $D_c$ [g cm$^{-3}$] | 1.886 | 1.884 | 2.118 |
| refls collected /$R_{int}$ | 60820/0.110 | 55336/0.083 | 15264 /0.079 |
| data / parameters | 16733 / 1192 | 19172 / 1192 | 9629 / 614 |
| $R_1(I \geq 2\sigma(I))$ /$wR_2$(all) | 0.059 / 0.139 | 0.053 / 0.115 | 0.077 / 0.186 |
| $\Delta\rho_{max / min}$ [e Å$^{-3}$] | 0.52 / -0.61 | 0.56 / -0.44 | 2.72 / –1.38 |
| CCDC | 2247739 | 2247740 | 2247741 |

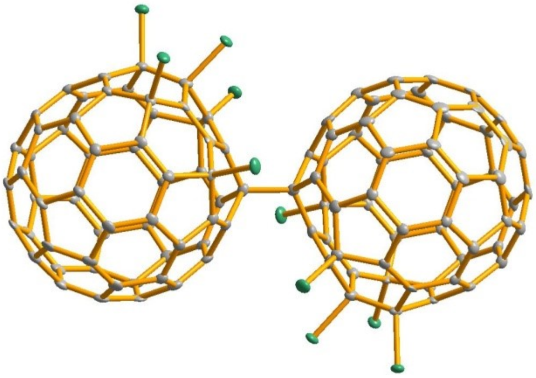

**Fig. *S*1.** Molecular structure of $(C_{60}Cl_5)_2$ (B1; isomer I) presented as an ORTEP projection (ellipsoid probability 50 %). Minor components of two disordered chlorine atoms (ca. 10 %) are not shown for clarity.

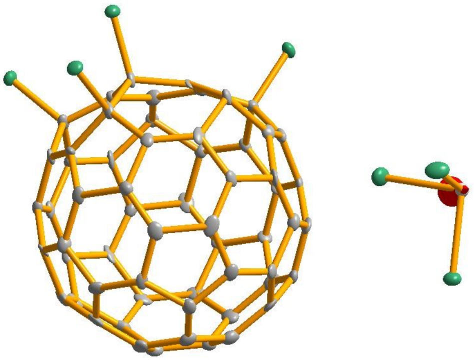

**Fig. *S*2.** Crystallographically independent units in the crystal structure of $(C_{60}Cl_4)_\infty \cdot SbCl_3$ presented as an ORTEP projection (ellipsoid probability 50 %).

A disorder in the crystal structures of $(C_{60}Cl_5)_2$ from batches B1 and B2 was interpreted as statistical distribution of three isomeric dimers of highly similar shape over the same crystallographic sites. All three isomers, I, II, and III, presented below as Schlegel diagrams in Fig. *S*3 share the addition pattern of the well-known $C_s$-$C_{60}Cl_6$ (skew pentagonal pyramid, SPP) and differ in through which positions the monomeric subunits are linked, i.e. which chlorine atom in the parent $C_{60}Cl_6$ is replaced with a $C_{60}$-$C_{60}$ bond.

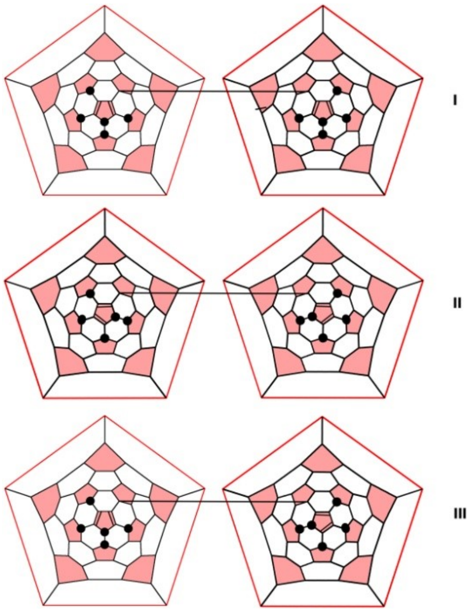

**Fig. *S3.*** Schlegel diagram representation of the connection of $C_{60}Cl_5$ units in the molecular structures of isomeric $(C_{60}Cl_5)_2$–I–III.

### EDX spectrometry

EDX and SEM analyses of the isolated compounds were carried out with the use of the FEI Nova NanoSEM 230 instrument equipped with a field-emission source with accelerating voltage of up to 30 kV adjustable with 0.1 kV accuracy and an energy dispersive X-ray detector Bruker XFlash 5010. Spectral processing was performed with the Esprit v 1.8 software. The results of Figs. *S*2 and *S*3 below reveal a reasonable agreement of the elemental composition with the findings of the single crystal X-ray crystallography. Thus, the EDX spectrum reveals the presence of carbon (91.5±10.5 at. %), chlorine (5.5±0.4 at. %), antimony (2.4±0.5 at. %), and oxygen (0.8±0.5 at. %). A small content of antimony (2.4%) in the $(C_{60}Cl_5)_2$ sample is likely due to the trace amounts of the products of hydrolysis of $SbCl_5$ that can occur during its addition into the reaction ampoule.

The EDX composition of the polymeric phase $(C_{60}Cl_4)_\infty$ (Fig. *S*3) is more consistent with the X-ray results. The major constituents are C (81.3±9.0 at. %), Cl (14.8±0.9 at. %), Sb (2.2±0.4 at. %), and admixtures of O (0.8±0.5 at. %) and Cu (0.9±0.1 at. %). The presence of copper is obviously due to the use of a copper plate as a sample holder in this case.

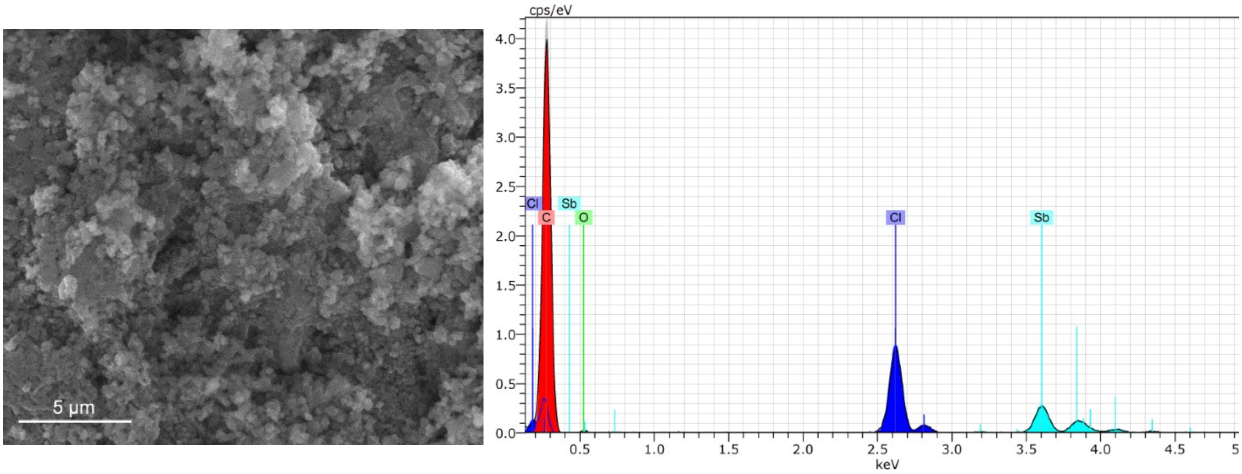

**Fig. *S*4.** SEM and EDX analysis of dimer $(C_{60}Cl_5)_2$.

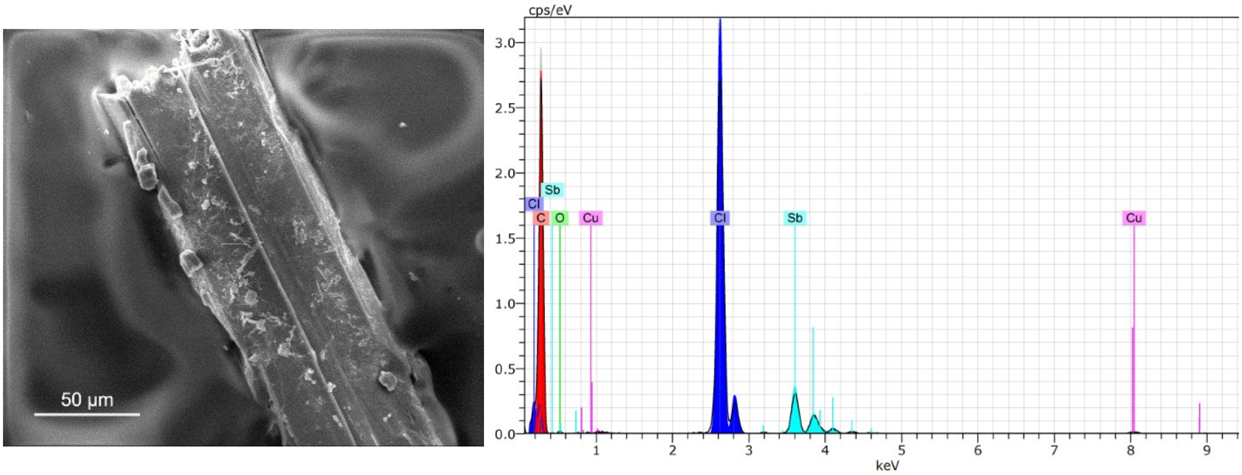

**Fig. *S*5.** SEM and EDX analysis of polymer $(C_{60}Cl_4)_\infty$.

## FTIR and Raman spectroscopy

FTIR spectra were recorded in KBr pellets in the range of 400–4000 cm$^{-1}$ (2 cm$^{-1}$ resolution) with the use of the FTIR Shimadzu IRAffinity-1 spectrometer.

The Raman spectra of the $(C_{60}Cl_5)_2$ and $(C_{60}Cl_4)_\infty$ crystals were acquired using a Renishaw InVia spectrometer with Leica DMLM optics (50x objective) under excitation with a 20 mW 633 nm He-Ne laser. In order to avoid damaging the crystals, the laser spot was defocused to ~100 µm and dimmed with neutral density filters to produce typical excitation power of ~$1\cdot10^{-4}$ mW/µm$^2$. To identify longitudinal modes in highly anisotropic polymer chains, polarized Raman scattering spectra were acquired in both parallel and perpendicular polarization modes with respect to the long crystal axis using a half-wave plate and polarizer crystals. The spectral data were processed with Renishaw Wire 3.4 software.

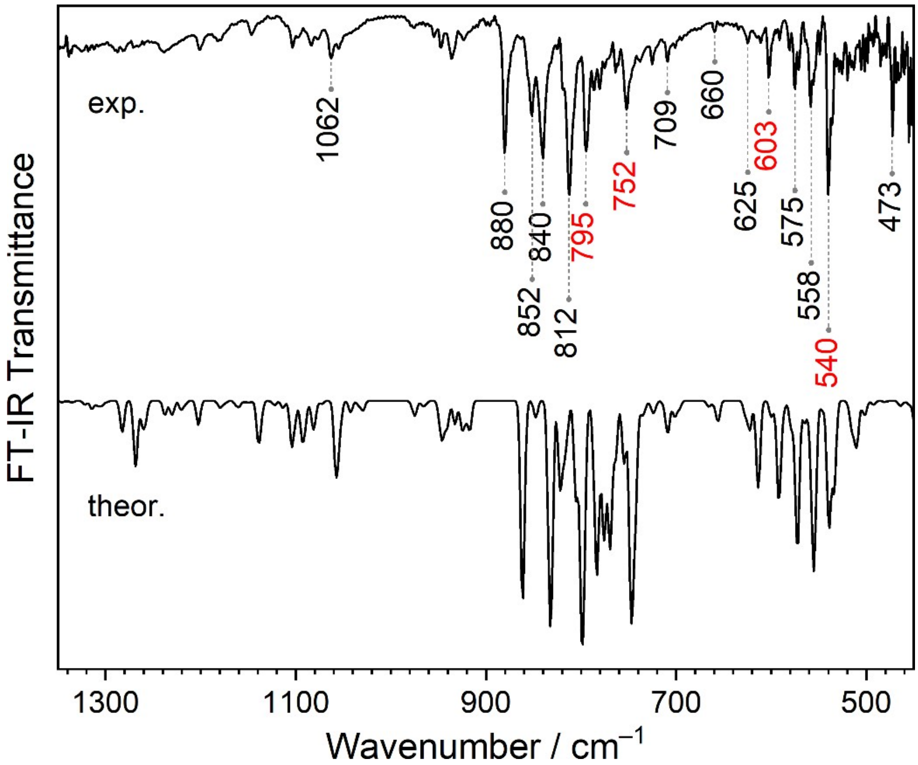

**Fig. *S*6**. FTIR spectra of dimer $(C_{60}Cl_5)_2$ (exp. – experimental spectrum recorded in KBr pellet, theor. – DFT calculated spectrum (PBE/TZP).

The FTIR spectrum of the dimer $(C_{60}Cl_5)_2$ (Fig. *S*4) features bands at 473, 540, 558, 569, 575, 603, 625, 660, 709, 752, 795, 812, 840, 852, 880, and 1062 cm$^{-1}$ and is in good agreement with the previously published data[S1] and the PBE/TZP calculations using the PRIRODA software.[S2-S4] The recorded and calculated Raman spectra of dimer $(C_{60}Cl_5)_2$ are presented in Fig. *S*5. The characteristic "dimeric" FTIR and Raman bands are marked with red. Most of the principal bands are shifted by just 3–5 cm$^{-1}$ with respect to $C_{60}Cl_6$. Previously, the presence of several additional bands was reported in ref. S5 for an unidentified red precipitate formed as an insoluble by-product in the synthesis of $C_s$-$C_{60}Cl_6$ by chlorination of $C_{60}$ with ICl.

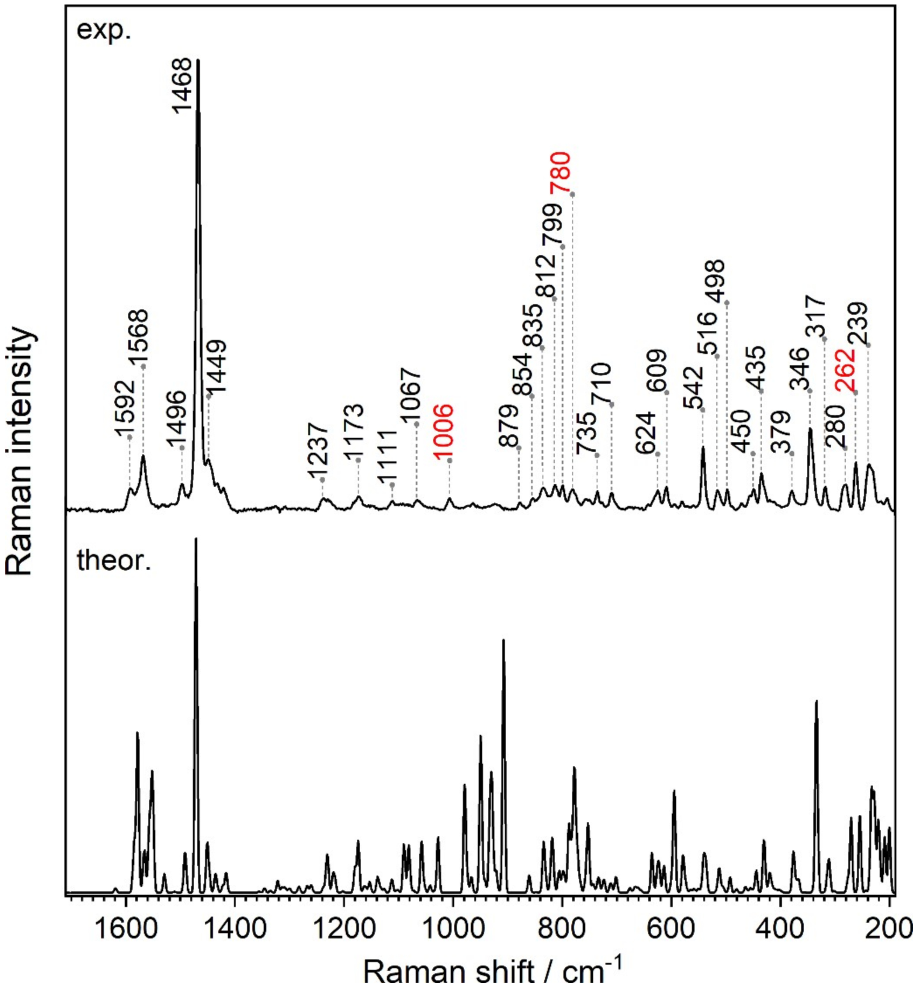

**Fig. *S*7.** Raman scattering spectra of dimer $(C_{60}Cl_5)_2$ (exp. – experimental spectrum, theor. – DFT calculated spectrum (PBE/TZP).

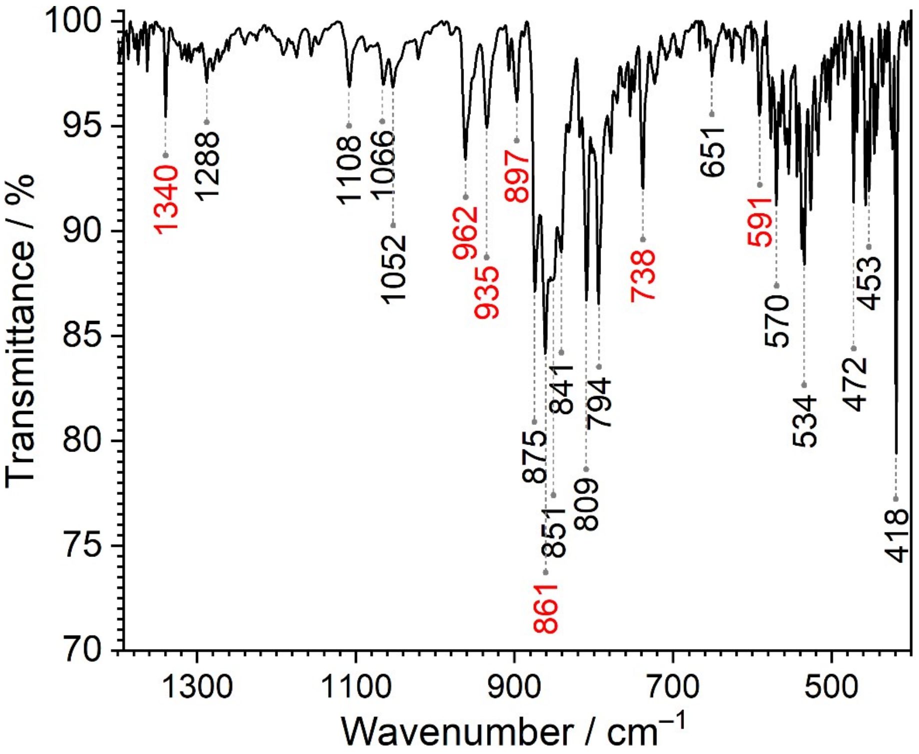

**Fig. *S*8.** FTIR spectrum of polymer $(C_{60}Cl_4)_\infty$ in KBr pellet.

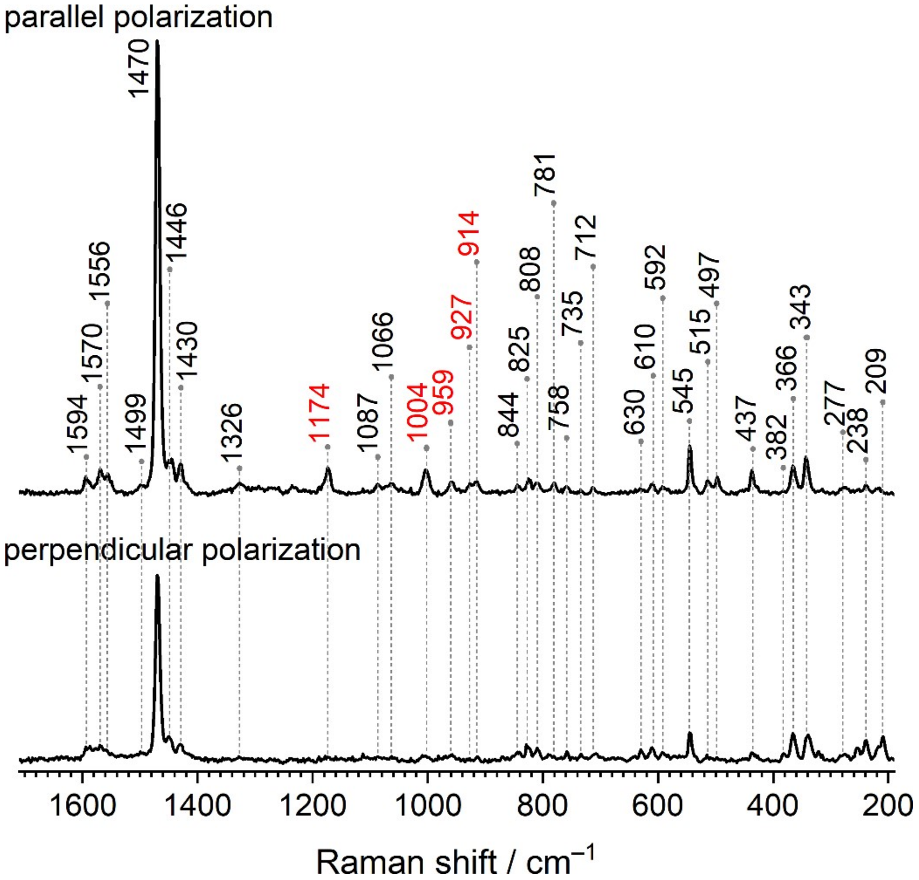

**Fig. *S*9.** Raman scattering spectra of polymer $(C_{60}Cl_4)_\infty$ in both parallel and perpendicular polarization to the long crystal axis.

The recorded FTIR spectrum (Fig. *S*6) of polymer $(C_{60}Cl_4)_\infty$ features principal bands at 418, 453, 472, 534, 570, 591, 651, 728, 794, 809, 841, 851, 861, 875, 897, 935, 962, 1052, 1066, 1108, 1288 and 1340 $cm^{-1}$.

### Thermal behavior of $(C_{60}Cl_4)_\infty$.

Thermogravimetric analysis (TGA) was carried out in the flow of nitrogen in the temperature range of 25–500 °C (10 °C $min^{-1}$ heating rate) using NETZSCH TG 209 F1 Iris instrument.

Experiments on thermal decomposition of $(C_{60}Cl_4)_\infty$·under inert atmosphere revealed its stability up to 260 °C (Fig. *S*8). The main decomposition step is observed between 300 and 450 °C, yet the completion of decomposition is still not reached at 500 °C. Additional experiments on decomposition under vacuum with IR-spectroscopic monitoring revealed that dechlorination to pristine $C_{60}$ can already be observed at the earliest decomposition stages.

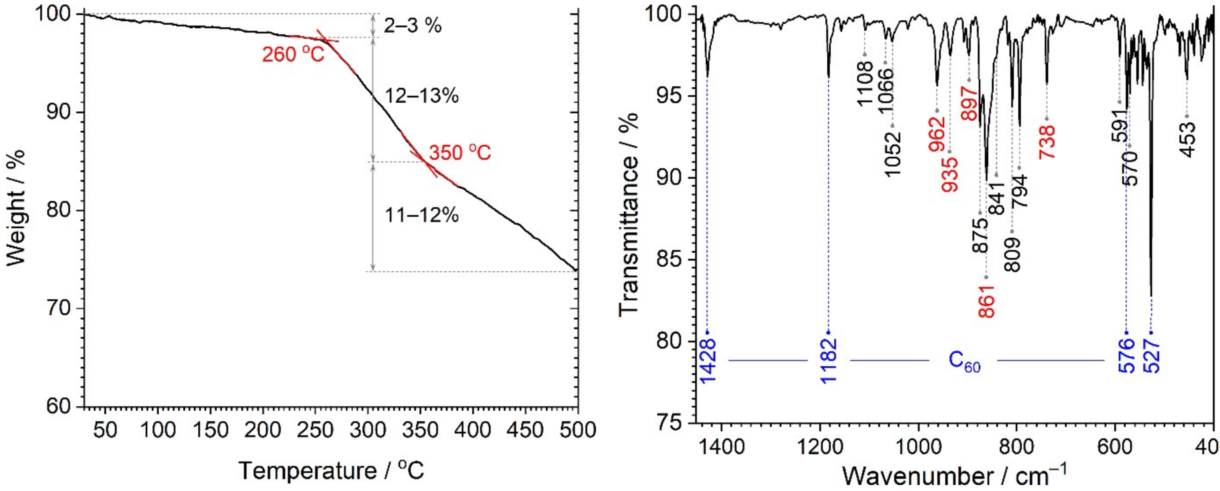

**Fig. *S*10.** TGA curve of $(C_{60}Cl_4)_\infty$ (left) and FTIR spectrum of the solid residue after heating of $(C_{60}Cl_4)_\infty$ under vacuum at 330 °C (right).

## Quantum-chemical calculations

The relative energy of the isomeric compounds was calculated at the RI-DFT level using the PRIRODA software[S2-S3]. The PBE exchange-correlation functional and a built-in gaussian basis set of TZ2P quality were employed[S4]. The computations of the IR and Raman spectra used a slightly more economic basis set of TZP quality. The vibrational frequencies and IR intensities were computed analytically, the Raman activities were obtained in a non-resonant approximation via numerical differentiation of the dipole moment derivatives with respect to the electric field.

## References

(S1) S. I. Troyanov and E. Kemnitz, *Chem. Commun.*, 2007, 2707.

(S2) D. N. Laikov, *Chem. Phys. Lett.* 2005, **416**, 116.

(S3) D. N. Laikov, *Chem. Phys. Lett.* 1997, **281**, 151.

(S4) Perdew, J. P.; Burke, K.; Ernzerhof, M. *Phys. Rev. Lett.* 1996, **77**, 3865.

(S5) I. V. Kuvychko, A. V. Streletskii, A. A. Popov, S. G. Kotsiris, T. Drewello, S. H. Strauss and O. V. Boltalina, *Chem. – Eur. J.,* 2005, **11**, 5426.